ChemComm

ROYAL SOCIETY OF CHEMISTRY

COMMUNICATION

View Article Online
View Journal | View Issue

Cite this: *Chem. Commun.*, 2020, **56**, 6440

Received 17th February 2020,
Accepted 29th April 2020

DOI: 10.1039/d0cc01234c

rsc.li/chemcomm

An enzyme-controlled Janus nanomachine for on-command dual and sequential release†

Ana M. Pérez-Calabuig,[a] Paula Díez,[a] Paloma Martínez-Ruiz,[a] Ramón Martínez-Máñez,[bcde] Alfredo Sánchez*[a] and Reynaldo Villalonga*[a]

A novel nanomachine for dual and sequential delivery of two different compounds was developed by grafting a thiol group and a pH sensitive β-cyclodextrin-based gate-like ensemble on acetylcholinesterase-modified Au–mesoporous silica Janus nanoparticles.

The design of advanced controlled release systems is a key research area in pharmaceuticals, cosmetics, agriculture and food industries.[1] Such systems, which allow the delivery of active compounds at the desired time and site and at a specific rate, can also improve the stability of the encapsulated substance.[2] For pharmacological applications, controlled delivery technology offers additional advantages including improved drug efficacy and bioavailability, reduced toxicity and enhanced patient compliance and convenience.[3] In this context, special efforts are currently devoted to designing stimulus-responsive carriers allowing on-command drug release in specific physiological environments.[4]

During the past few years, nanomaterials have been explored to develop controlled delivery systems with nanosized dimensions and improved release properties.[5] In particular, mesoporous silica nanoparticles (MSNs) have been widely used as nanocarriers for stimulus-responsive delivery due to their large loading capacity and easy functionalization with stimuli-sensitive gate-like ensembles.[6] With the aim to construct more sophisticated mesoporous nanocarriers for delivery applications, we previously reported a mask-protecting approach for the toposelective modification of MSNs with Au nanoparticles.[7] The resulting Janus colloids allowed construction of nanomachines through the stable immobilization of enzymes on the metal surface.[8] These biocatalysts can act as sensing-effector elements able to control the opening mechanism of stimulus-sensitive molecular or supramolecular ensembles on the mesoporous face, thus provoking the release of the encapsulated cargo.[9]

In this work, we describe the design of an original enzyme-controlled nanomachine for the on-command dual and sequential delivery of two different compounds, using tris(bipyridine)ruthenium(II) chloride ($Ru(bipy)_3Cl_2$) and Azure A as model cargos. The proposed design involves the use of Au–MSN Janus nanoparticles as ''hardware'' to assemble the nanodevice and the enzyme acetylcholinesterase (EC 3.1.1.7) as a sensing-effector element immobilized on the metal nanoparticle face. Moreover, the MSN face was employed as a nanocontainer for loading $Ru(bipy)_3Cl_2$ as the encapsulated cargo and was further mechanized with a thiol-responsive β-cyclodextrin-based molecular gate. The attached β-cyclodextrin (CD) moieties were also employed as supramolecular hosts for the formation of pH-sensitive inclusion complexes with Azure A.

As illustrated in Fig. 1, we envisioned that the device (solid S_2) will be fuelled by either acetylcholine or acetylthiocholine, two common substrates for the controlling enzyme.[10] In the absence of such compounds, the nanomachine will show negligible or zero-release. However, the addition of acetylcholine as a chemical input signal will lead to the production of choline and acetic acid through the enzyme-catalyzed hydrolysis of this substrate. This enzymatic transformation will cause a pH drop leading to the protonation of Azure A, with the consequent dethreading of its inclusion complex with CD and release of the thiazine dye. On the other hand, the use of acetylthiocholine as a trigger will produce thiocholine and acetic acid upon enzymatic transformation on the nanoparticle surface. These products will lead to the simultaneous disruption of the pH-sensitive CD-based host–guest complex and the

[a] *Nanosensors and Nanomachines Group, Department of Analytical Chemistry, Faculty of Chemistry, Complutense University of Madrid, Madrid 28040, Spain. E-mail: alfredos@ucm.es, rvillalonga@quim.ucm.es*
[b] *Instituto Interuniversitario de Investigación de Reconocimiento Molecular y Desarrollo Tecnológico (IDM), Universitat Politècnica de València, Universitat de València, Camino de Vera s/n, Valencia 46022, Spain*
[c] *Unidad Mixta UPV-CIPF de Investigación en Mecanismos de Enfermedades y Nanomedicina, Valencia, Universitat Politècnica de València, Centro de Investigación Príncipe Felipe, València, Spain*
[d] *CIBER de Bioingeniería, Biomateriales y Nanomedicina (CIBER-BBN), Spain*
[e] *Unidad Mixta de Investigación en Nanomedicina y Sensores, Universitat Politècnica de València, IIS La Fe, Valencia, Spain*

† Electronic supplementary information (ESI) available: Experimental part and characterization experiments. See DOI: 10.1039/d0cc01234c

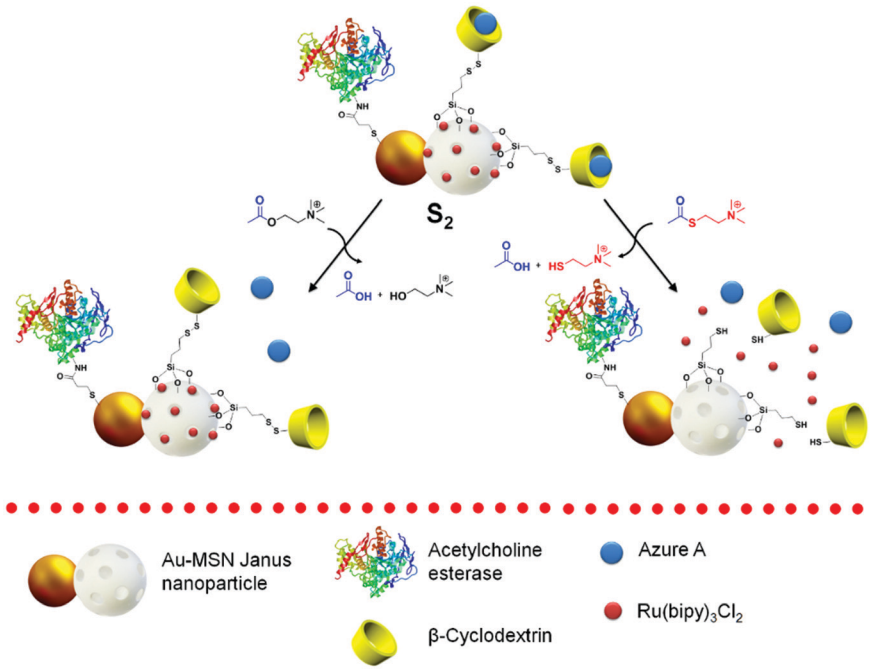

Fig. 1 Performance of the enzyme-controlled Janus nanomachine for single delivery of Azure A in the presence of acetylcholine (left) and dual delivery of $Ru(bipy)_3Cl_2$ and Azure A in the presence of acetylthiocholine (right).

thiol-responsive gate-like ensemble on the nanoparticle pores, with a consequent dual release of Azure A and the encapsulated $Ru(bipy)_3Cl_2$. In contrast with our previous works,[8,9] this novel multi-stimuli responsive nanodevice controlled by a single enzyme allows the on-command release of two different cargos by proper selection of the trigger compounds. This nanodevice also allows programming the release sequence, which is relevant for therapeutic strategies in which a single drug should be administered in two dosage phases, or two different drugs should be sequentially administered over time.

As represented in Scheme S1 in the ESI,† the construction of this nanodevice implied the initial preparation of Au–MSN Janus nanoparticles (solid S_0) as previously described (see ESI† for details).[7] This nanoparticle was then modified at the Au face with 3-mercaptopropionic acid (MPA) to protect the metal surface and allow further covalent immobilization of acetylcholinesterase. Although further displacement of MPA by a bulky silane derivative is not favored due to steric hindrance, a 10-fold molar excess of MPA (1.1 mmol) *vs.* total Au was employed to ensure formation of a compact self-assembled monolayer. To assemble the gating mechanism, 3-mercaptopropyltrimethoxysilane was then attached to the mesoporous nanoparticle face and the porous nanomaterial was further loaded with $Ru(bipy)_3Cl_2$. The modified nanoparticle was then capped with a thiol-sensitive molecular gate by treatment with a β-cyclodextrin methanethiosulfonate derivative (solid S_1).

The resulting nanoparticles were characterized by different techniques. As can be observed from Fig. S1 in the ESI,† the nanoparticles showed a quasi-spherical morphology with an average size (±SD, n = 100) of 102 ± 16 nm, retaining the Janus-type morphology with opposite Au and mesoporous faces after dye loading and chemical modification, as revealed by TEM analysis.

The N_2 adsorption–desorption isotherms of the Janus colloids (solid S_0) showed the characteristic type IV pattern of mesoporous materials, with an adsorption step at intermediate P/P_0 values around 0.1–0.3 (Fig. S2 in ESI†). The total specific surface area of this solid was calculated as 837 $m^2\ g^{-1}$ by applying the BET model. In addition, a pore volume of 0.94 $cm^3\ g^{-1}$ and a pore size of 2.5 nm were estimated for this initial nanomaterial. In contrast, the N_2 adsorption–desorption isotherms for the $Ru(bipy)_3Cl_2$ loaded and capped nanomaterial (solid S_1) are typical of mesoporous materials with filled pores, with a significant reduction in the adsorbed N_2 volume and a total specific surface area of 141 $m^2\ g^{-1}$. No appreciable porosity was determined for this nanomaterial by using the BET model, suggesting a high loading of the cargo into the mesopores.

X-ray diffraction patterns of the starting Janus nanoparticles (solid S_0) and the functionalized derivative (solid S_1) showed a low-angle reflection around 2.4°–2.6°, corresponding to the (100) Bragg peak for an MCM41-type structured hexagonal ordered array of pores (Fig. S3 in ESI†).[7b] The small shift observed for this peak for S_1 is ascribed to the anchored MPA groups,[11] demonstrating the chemical functionalization of the starting nanoparticles. These nanomaterials also showed the cubic gold characteristic (111), (200), (220) and (311) diffraction peaks. These results suggest that the nanoparticle retained the Au–MSN Janus architecture after functionalization, as observed by TEM.

FT-IR analysis confirmed the dye loading and functionalization of solid S_1 (Fig. S4 in ESI†). Both the raw and modified Janus colloids showed the characteristic absorption bands of siliceous materials at 463 cm^{-1}, 960 cm^{-1} and 1080 cm^{-1}

attributed to the vibration of the Si–O, Si–OH and Si–O–Si bonds, respectively.[12] In addition, the broad band around 3400 cm^{-1} can be ascribed to the O–H bonding vibration of the SiO–H groups and adsorbed water molecules. The spectrum of solid S_1 showed a large band at 1630 cm^{-1}, which can be ascribed to the vibration of the $-CO_2^-$ groups from the aliphatic acid moieties attached to the Au nanoparticle surface. The absorption band at 2933 cm^{-1}, corresponding to the stretching vibrations of the $-CH_2$ groups, also confirmed functionalization of this nanomaterial with aliphatic ligands both at the metal and mesoporous faces. Loading of $Ru(bipy)_3Cl_2$ in solid S_1 was confirmed by a characteristic band at 1410 cm^{-1}.[13] On the other hand, the total alkaline hydrolysis of solid S_1 revealed a $Ru(bipy)_3Cl_2$ content of 12 μmol g^{-1} nanoparticle.

To assemble the enzyme-controlled nanomachine S_2, the enzyme acetylcholinesterase was attached to the Au nanoparticle face using 1-ethyl-3-(3-dimethylaminopropyl)carbodiimide and *N*-hydroxysuccinimide as coupling agents. Finally, the resulting solid was incubated in an aqueous solution of Azure A to allow the formation of supramolecular complexes between the dye and the grafted CD moieties. The total content of Azure A in the resulting solid was estimated to be 80 μmol g^{-1} by UV/vis spectroscopy. Enzymatic assays revealed a content of 56 U g^{-1} acetylcholinesterase in the solid S_2.

The capacity of the nanomachine to deliver the encapsulated compounds upon addition of the trigger enzyme substrates was measured by using UV/vis spectroscopy. Fig. S5 in the ESI† shows the spectra of the solutions after 1 h of incubation of S_2 in the presence of the trigger compounds at 150 mM final concentration. In the absence of the enzyme substrates, a negligible release of the encapsulated compounds was observed. In contrast, the presence of acetylcholine results in the release of Azure A, as confirmed by the broad absorption band around 620 nm (for reference see Fig. S6 in ESI†). No appreciable increase in the absorbance around 454 nm was observed, suggesting that the nanomachine remains capped with the thiol-sensitive gate-like ensemble upon addition of acetylcholine, and accordingly, $Ru(bipy)_3Cl_2$ was not released.

On the other hand, a noticeable absorption band around 454 nm was observed in the experiments where acetylthiocholine was added to the incubation media. This fact suggests the disruption of the thiol-sensitive linkages at the mesoporous nanoparticle surface and the release of the encapsulated $Ru(bipy)_3Cl_2$. A large increase in the intensity of the band at 620 nm and the appearance of a shoulder band around 590 nm were also observed. The increased absorbance intensity could be mainly caused by the enzymatic production of acetic acid through the enzyme-catalyzed hydrolysis of the substrate, leading to the protonation of Azure A and disruption of the host–guest complexes with the CDs. In addition, the thiol-induced dissociation of the gate-like ensemble on S_2 led to the release of non-dissociated CD–Azure A complexes, which have different absorption patterns to that of the free thiazine dye (Fig. S7 in ESI†), thus increasing the overall absorption intensity and producing a shoulder band.

Kinetics release assays were performed to further confirm the functional mechanism of the nanomachine. In a typical assay, the enzyme substrates acetylcholine or acetylthiocholine at 150 mM were used as input signals. This high concentration was employed to ensure maximum dye release, although acetylcholine or acetylthiocholine was able to trigger the release mechanism at lower concentrations of 10 mM and 25 mM, respectively (Fig. S8 in ESI†). As a blank experiment, S_2 was incubated over time without the enzyme substrates. As a positive control, *N*-acetyl cysteine at 150 mM was employed due to its capacity to disrupt both the pH-sensitive CD-based supramolecular complexes and the thiol-responsive molecular gates on the nanomachine.

Fig. 2A shows the time-course of Azure A release from the mechanized nanoparticle in the presence and absence of the enzyme substrates. No appreciable dye release was observed in the control experiment, but a fast increase in the absorbance at 620 nm was observed after adding acetylcholine, reaching a saturation value 90 min after addition. These results support our hypothesis on the recognition of the trigger by the controlling enzyme acetylcholinesterase, leading to the enzymatic production of acetic acid and the reduction in the pH of the incubation solution. Such an acidic environment causes protonation of the Azure A molecules included into the cavity of CDs, leading to dethreading of the inclusion complex and dye delivery. A higher delivery was noticed on using acetylthiocholine as the chemical input signal, due to the enzymatic production of thiocholine

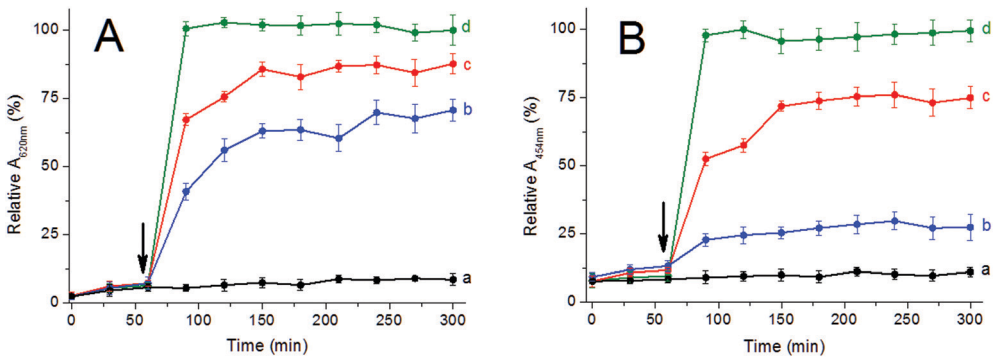

Fig. 2 Kinetics of Azure A (A) and $Ru(bipy)_3Cl_2$ (B) release from S_2 in 20 mM Na_2SO_4, pH 7.5 in the absence (a) and the presence of 150 mM acetylcholine (b), acetylthiocholine (c) and *N*-acetyl cysteine (d). Triggers were added after 1 h of incubation.

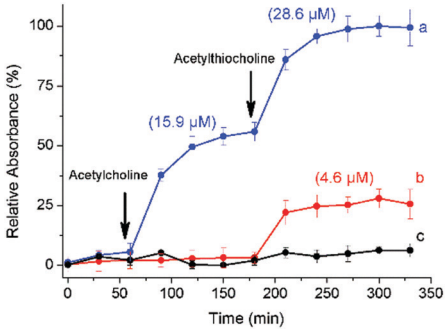

Fig. 3 Kinetics of Azure A (a) and $Ru(bipy)_3Cl_2$ (b) release from S_2 in 20 mM Na_2SO_4, pH 7.5 after sequential addition of acetylcholine and acetylthiocholine at 150 mM final concentration. Blank experiment without trigger addition (c). 100% represents the maximum amount of dye released. Maximum concentration of dye released at each stage is shown in parentheses.

allowing the dissociation of the thiol-sensitive gate ensemble on S_2 and the release of CD–Azure A complexes to the incubation solution. A faster kinetics and large delivery were observed in the presence of *N*-acetyl cysteine, because this compound could not be enzymatically transformed to provide free thiol and carboxylic acid groups to the mechanized nanoparticle.

The kinetics for $Ru(bipy)_3Cl_2$ release from the S_2 samples is shown in Fig. 2B, with a negligible increase in the absorbance at 454 nm in the absence of triggers. Only a slight increase in the analytical signal was noticed on addition of acetylcholine to the incubation solution, probably caused by the overlapping of the absorption band from the pH-induced release of Azure A. In contrast, a fast increase in the absorbance at 454 nm was observed after addition of acetylthiocholine, suggesting that the enzyme-mediated production of thiocholine allows the disassembly of the thiol-sensitive molecular gate on the pore surface and the release of the encapsulated $Ru(bipy)_3Cl_2$. As expected, an improved delivery pattern was observed on using *N*-acetyl cysteine as the trigger. It should be highlighted that no appreciable release was observed from S_2 after thermal inactivation of the enzyme and further incubation with the triggers (Fig. S9 in ESI†), thus demonstrating that acetylcholinesterase is essential for the release mechanism.

To provide insight into the possibilities of this enzyme-controlled nanomachine, its capacity for sequential release was finally tested (see Scheme S2 in the ESI†). As illustrated in Fig. 3, addition of acetylcholine caused a partial delivery of the supramolecularly encapsulated Azure A dye (20.3% of the total encapsulated dye) without a noticeable release of $Ru(bipy)_3Cl_2$. Further addition of acetylthiocholine promoted the release of $Ru(bipy)_3Cl_2$ from the mesopores, reaching about 38.3% of the total encapsulated dye. Addition of acetylthiocholine also led to a more complete delivery of Azure A, free and associated with CDs, reaching 35.8% of the total encapsulated dye.

In summary, we have described here for the first time the construction of a novel Janus nanomachine provided with enzymatic control and stimulus-responsive release mechanisms for the dual delivery of two different compounds by selective fuelling with enzyme substrates. This nanodevice also allowed the time-controlled sequential delivery of the encapsulated payloads.

We believe that the use of different enzymes on mesoporous Janus nanoparticles mechanized with a variety of stimulus-responsive ensembles will open up new possibilities for the design of advanced nanodevices for on-command programmed sequential delivery, with high impact in pharmaceuticals and other industries.

This work was supported by CTQ2017-87954-P and RTI2018-100910-B-C41 grants from the Spanish Ministry of Economy and Competitiveness and PROMETEO2018/024 from the Generalitat Valenciana.

Conflicts of interest

There are no conflicts to declare.

Notes and references

1 (*a*) X. Zhang, L. Han, M. Liu, K. Wang, L. Tao, Q. Wan and Y. Wei, *Mater. Chem. Front.*, 2017, **1**, 807; (*b*) M. Saifullah, M. R. I. Shishir, R. Ferdowsi, M. R. T. Rahman and Q. Van Vuong, *Trends Food Sci. Technol.*, 2019, **86**, 230.
2 A. M. Bakry, S. Abbas, B. Ali, H. Majeed, M. Y. Abouelwafa, A. Mousa and L. Liang, *Compr. Rev. Food Sci. Food Saf.*, 2016, **15**, 143.
3 N. Kamaly, B. Yameen, J. Wu and O. C. Farokhzad, *Chem. Rev.*, 2016, **116**, 2602.
4 (*a*) C. Ding, Y. Liu, T. Wang and J. Fu, *J. Mater. Chem. B*, 2016, **4**, 2819; (*b*) K. K. Bawa and J. K. Oh, *Mol. Pharmacol.*, 2017, **14**, 2460.
5 (*a*) M. Martínez-Ballesta, A. Gil-Izquierdo, C. García-Viguera and R. Domínguez-Perles, *Foods*, 2018, **7**, 72; (*b*) E. Keles, Y. Song, D. Du, W. J. Dong and Y. Lin, *Biomater. Sci.*, 2016, **4**, 1291.
6 (*a*) D. Tarn, D. P. Ferris, J. C. Barnes, M. W. Ambrogio, J. F. Stoddart and J. I. Zink, *Nanoscale*, 2014, **6**, 3335; (*b*) Y. L. Zhao, Z. Li, S. Kabehie, Y. Y. Botros, J. F. Stoddart and J. I. Zink, *J. Am. Chem. Soc.*, 2010, **132**, 13016; (*c*) P. Díez, A. Sánchez, C. D. L. Torre, M. Gamella, P. Martínez-Ruíz, E. Aznar, R. Martínez-Máñez, J. M. Pingarrón and R. Villalonga, *ACS Appl. Mater. Interfaces*, 2016, **8**, 7657.
7 (*a*) A. Sánchez, P. Díez, P. Martínez-Ruíz, R. Villalonga and J. M. Pingarrón, *Electrochem. Commun.*, 2013, **30**, 51; (*b*) R. Villalonga, P. Díez, A. Sánchez, E. Aznar, R. Martínez-Máñez and J. M. Pingarrón, *Chem. – Eur. J.*, 2013, **19**, 7889.
8 (*a*) P. Díez, A. Sánchez, M. Gamella, P. Martínez-Ruíz, E. Aznar, C. De La Torre, J. R. Murguía, R. Martínez-Máñez, R. Villalonga and J. M. Pingarrón, *J. Am. Chem. Soc.*, 2014, **136**, 9116; (*b*) A. Llopis-Lorente, B. De Luis, A. García-Fernández, P. Díez, A. Sánchez, M. D. Marcos, R. Villalonga, R. Martínez-Máñez and F. Sancenón, *J. Mater. Chem. B*, 2017, **5**, 6734; (*c*) A. Llopis-Lorente, P. Díez, A. Sánchez, M. D. Marcos, F. Sancenón, P. Martínez-Ruiz, R. Villalonga and R. Martínez-Máñez, *Nat. Commun.*, 2017, **8**, 1.
9 (*a*) S. Jimenez-Falcao, N. Joga, A. García-Fernández, A. Llopis-Lorente, D. Torres, B. De Luis, F. Sancenón, P. Martínez-Máñez, R. Martínez-Máñez and R. Villalonga, *J. Mater. Chem. B*, 2019, **7**, 4669; (*b*) A. Llopis-Lorente, A. García-Fernández, E. Lucena-Sánchez, P. Díez, F. Sancenón, R. Villalonga, D. A. Wilson and R. Martínez-Máñez, *Chem. Commun.*, 2019, **55**, 13164; (*c*) T. M. Godoy-Reyes, A. Llopis-Lorente, A. García-Fernández, P. Gaviña, A. M. Costero, R. Villalonga, F. Sancenón and R. Martínez-Máñez, *Org. Chem. Front.*, 2019, **6**, 1058.
10 P. Zdražilová, Š. Štěpánkova, M. Vránova, K. Komers, A. Komersová and A. Čegan, *Z. Naturforsch., C: J. Biosci.*, 2006, **61**, 289.
11 D. Das, J. F. Lee and S. Cheng, *J. Catal.*, 2004, **223**, 152.
12 M. Stefanescu, M. Stoia and O. Stefanescu, *J. Sol-Gel Sci. Technol.*, 2007, **41**, 71.
13 R. B. Dyer, K. M. Omberg, R. M. Leasure, T. J. Meyer, J. R. Schoonover and J. A. Treadway, *J. Am. Chem. Soc.*, 2002, **119**, 7013.

Electronic Supplementary Information

Enzyme-controlled Janus nanomachine for on-command dual and sequential release

Ana M. Pérez-Calabuig,[a] Paula Díez,[a] Paloma Martínez-Ruiz,[a] Ramón Martínez-Máñez,[b,c,d,e] Alfredo Sánchez,*[a] Reynaldo Villalonga*[a]

[a]Nanosensors and Nanomachines Group, Department of Analytical Chemistry, Faculty of Chemistry, Complutense University of Madrid, 28040 Madrid, Spain. E-mail: alfredos@ucm.es, rvillalonga@quim.ucm.es

[b]Instituto Interuniversitario de Investigación de Reconocimiento Molecular y Desarrollo Tecnológico (IDM), Universitat Politècnica de València, Universitat de València, Camino de Vera s/n, 46022, Valencia, Spain

[c]Unidad Mixta UPV-CIPF de Investigación en Mecanismos de Enfermedades y Nanomedicina, Valencia, Universitat Politècnica de València, Centro de Investigación Príncipe Felipe, València, Spain.

[d]CIBER de Bioingeniería, Biomateriales y Nanomedicina (CIBER-BBN).

[e]Unidad Mixta de Investigación en Nanomedicina y Sensores. Universitat Politècnica de València, IIS La Fe, Valencia, Spain

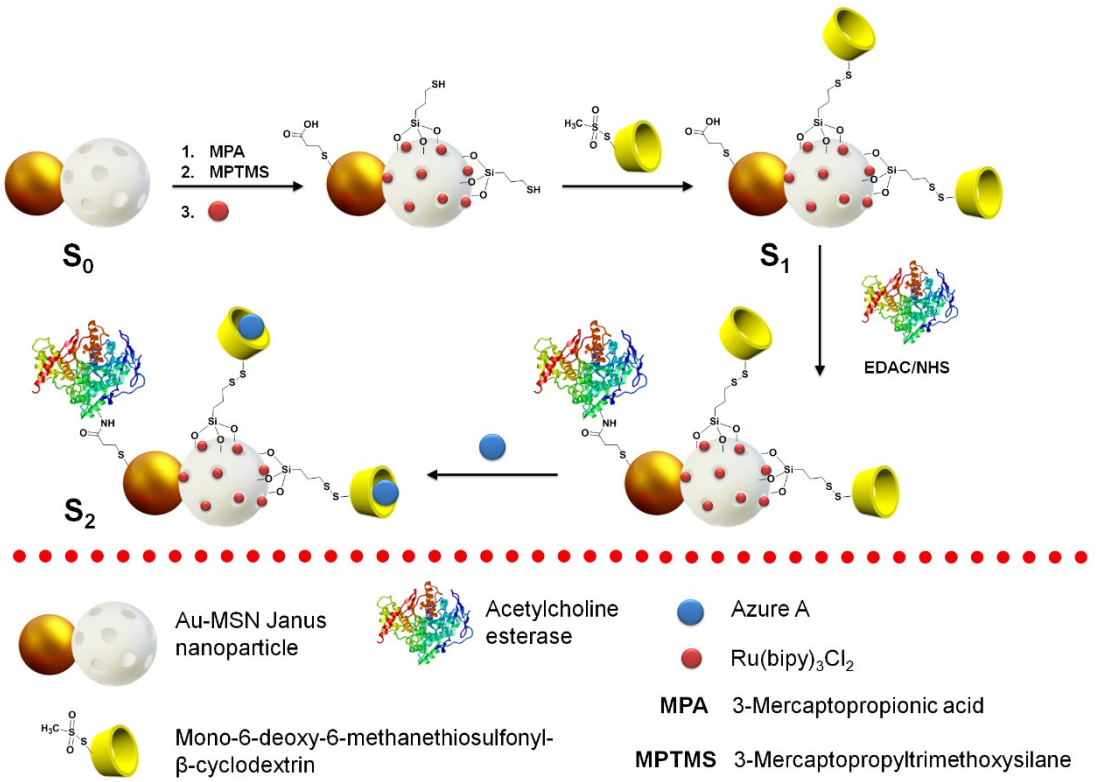

Scheme 1S. Schematic display of the processes involved in the preparation of the acetylcholine esterase-controlled nanomachine $\mathbf{S_2}$.

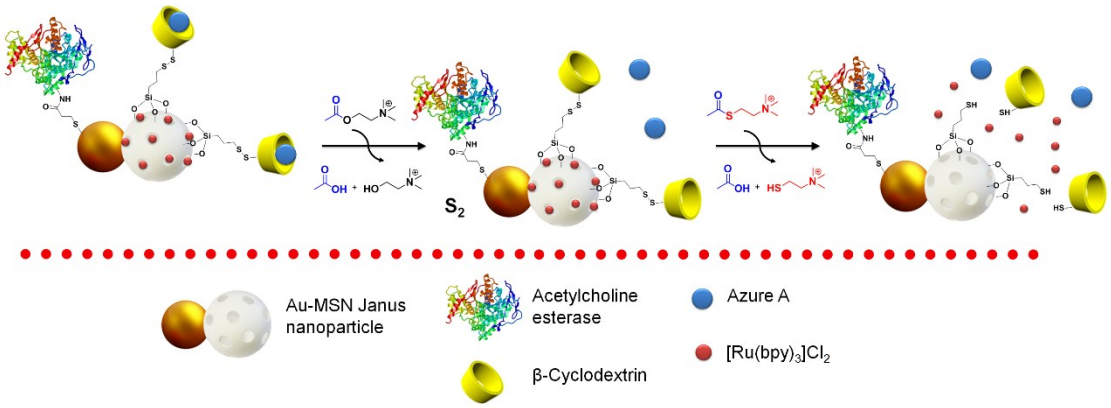

Scheme 2S. Performance of the enzyme-controlled Janus nanomachine for sequential delivery.

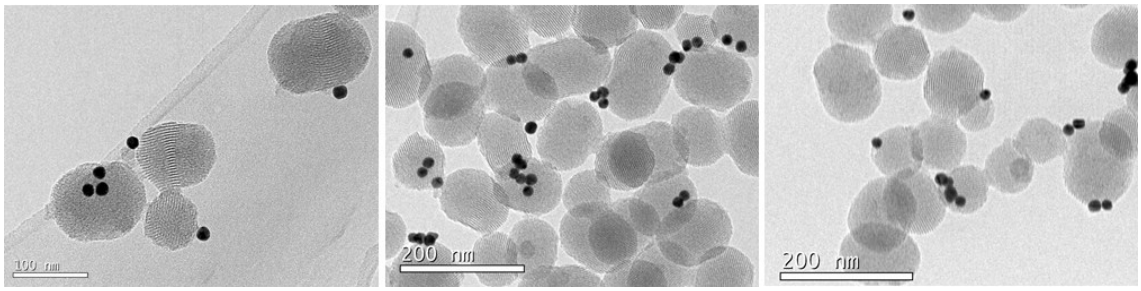

Figure 1S. Representative TEM images of solid $\mathbf{S_1}$.

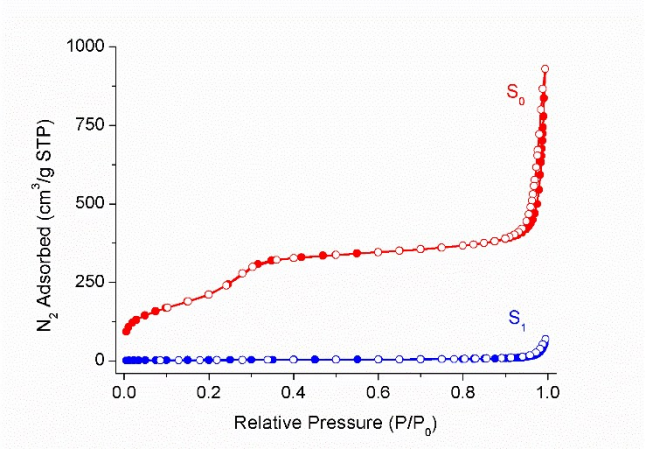

Figure 2S. Nitrogen adsorption (closed)/desorption (open) isotherms for solids $\mathbf{S_0}$ and $\mathbf{S_1}$.

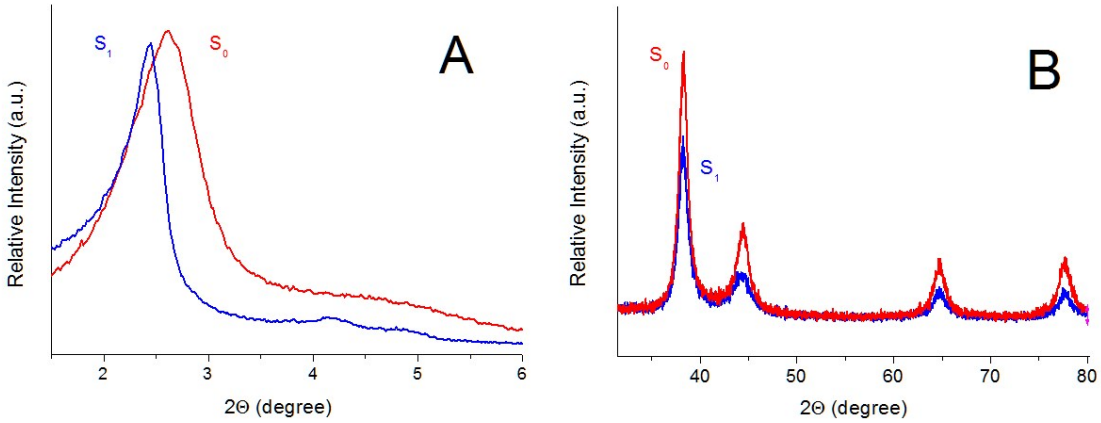

Figure 3S. Powder X-ray diffraction analysis for solids $\mathbf{S_0}$ and $\mathbf{S_1}$ at low (A) and high (B) diffraction angles.

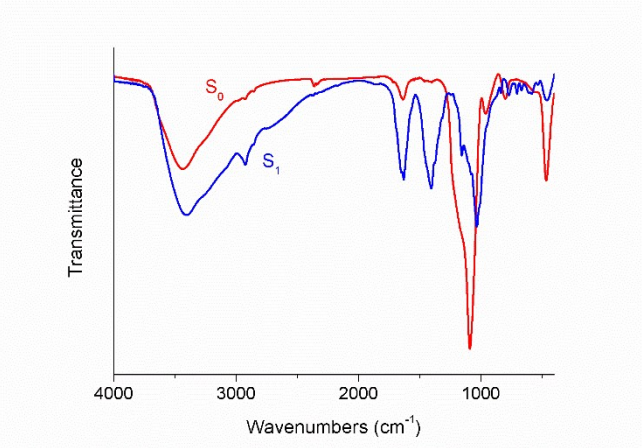

Figure 4S. FT-IR analysis for solids $\mathbf{S_0}$ and $\mathbf{S_1}$.

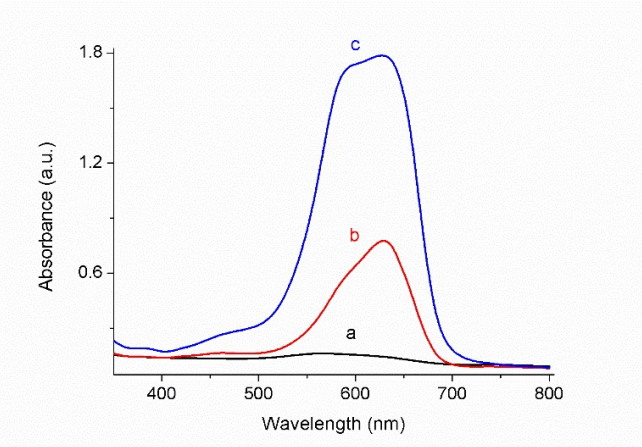

Figure 5S. UV/VIS spectra for $\mathbf{S_2}$ dispersion in 20 mM Na_2SO_4, pH 7.5 after 1 h incubation in the absence (a) and the presence of 150 mM acetylcholine (b) or acetylthiocholine (c).

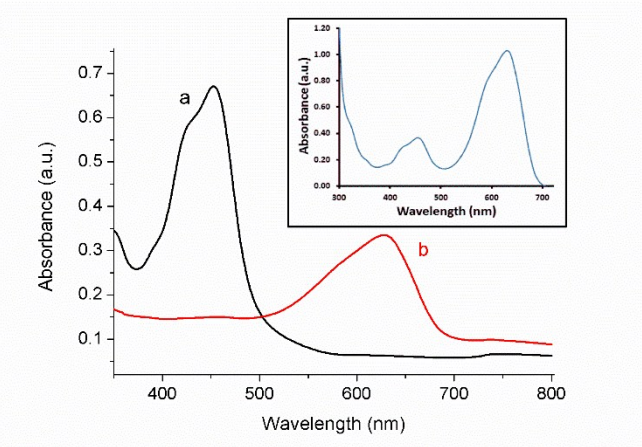

Figure 6S. UV/VIS spectra for 47 µM $Ru(bipy)_3Cl_2$ (a) and 5 µM Azure A (b) solutions in 20 mM Na_2SO_4, pH 7.5. Inset: UV/Vis spectrum for a mixture of 21 µM $Ru(bipy)_3Cl_2$ and 17 µM Azure A (b) in 20 mM Na_2SO_4, pH 7.5.

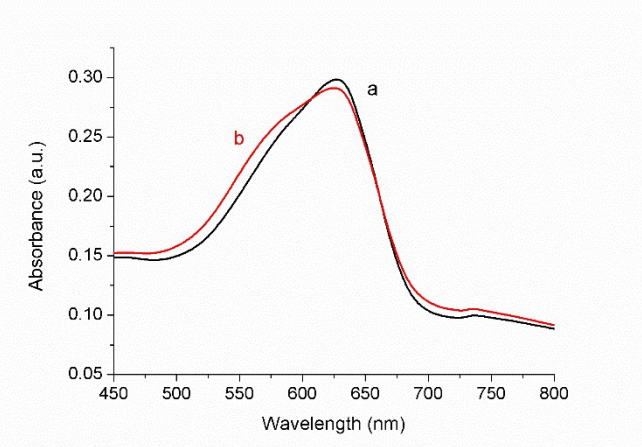

Figure 7S. VIS spectra for 5 µM Azure A solution in 20 mM Na_2SO_4, pH 7.5 before (a) and after addition of CD at 100 µM (b)

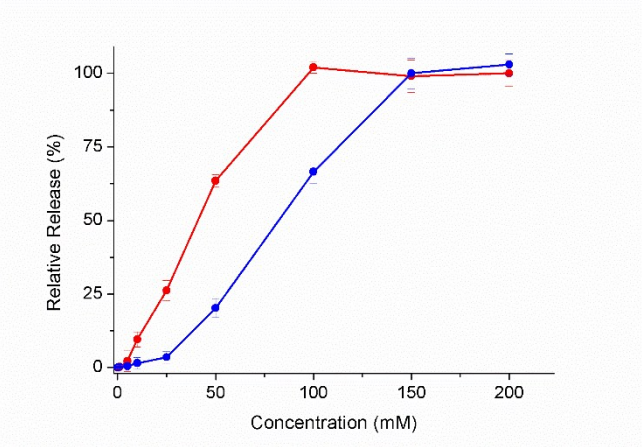

Figure 8S. Relative release of Azure A (blue) and $Ru(bipy)_3Cl_2$ (red) from **S_2** in 20 mM Na_2SO_4, pH 7.5 in the presence of 150 mM acetylcholine and 150 mM acetylthiocholine, respectively.

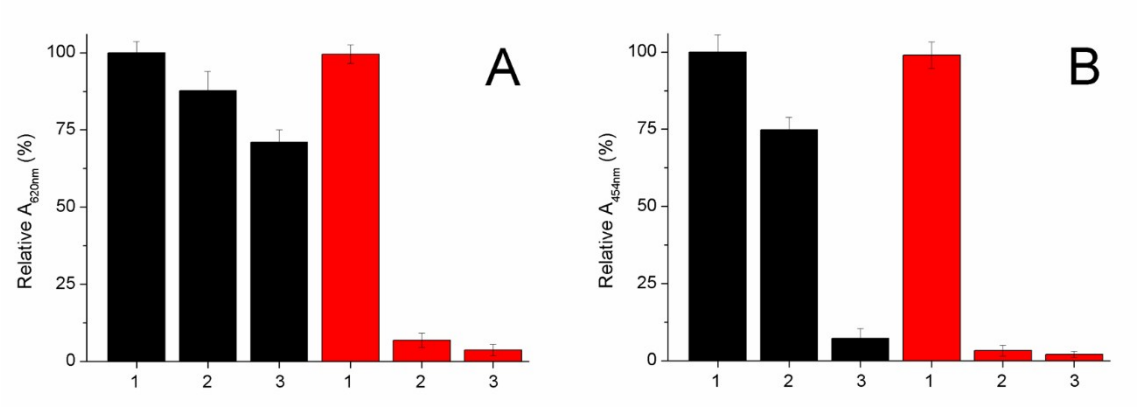

Figure 9S. Relative release of Azure A (A) and $Ru(bipy)_3Cl_2$ (B) from **S_2** (black) and thermal inactivated **S_2** (red) in 20 mM Na_2SO_4, pH 7.5 in the presence of 150 mM N-acetyl cysteine (1) acetylthiocholine (2) and acetylcholine (3).

1. Experimental Part

1.1. Chemicals

Tetraethoxysilane, cetyltrimethylammonium bromide, β-cyclodextrin, $NaSSO_2CH_3$, $HAuCl_4$, (3-mercaptopropyl) trimethoxysilane, 3-mercaptopropionic acid, tris(2,2′-bipyridyl)dichlororuthenium(II) hexahydrate, Azure A hydrochloride, acetylthiocholine chloride, acetylcholine chloride, acetylcholine esterase, 5,5′-dithiobis(2-nitrobenzoic acid) and p-toluenesulfonyl chloride were purchased from Sigma-Aldrich. Solvents were provided by Scharlau. All other reagents were of analytical grade.

1.2. Instruments and general techniques

Transmission electron microscopy (TEM) measurements were performed with a JEOL JEM-2100 microscope. Spectrophotometric measurements were performed using an Ultrospec 8000 UV/VIS spectrophotometer. Powder X-ray diffraction was performed with an X'Pert MRD diffractometer. Nitrogen adsorption/desorption isotherms and pore size distributions were determined with a Micromeritics ASAP 2020 automated analyzer. FT-IR spectra were obtained from KBr discs by using a Nicolet Nexus 670/870 spectrometer. ^{1}H-NMR analysis was performed with a Bruker AV 500MHz instrument. Acetylcholine esterase activity was determined by using acetylthiocholine as substrate in 10 mM sodium carbonate buffer, pH 10 at 25ºC.[1] The enzymatic product was detected at 412 nm after reaction with 5,5′-dithiobis(2-nitrobenzoic acid) (Ellman reagent). One unit was defined as the amount of enzyme able to release 1.0 μmol thiocholine per minute under the cited conditions.

1.3. Synthesis of mono-6-deoxy-6-methanethiosulfonyl-β-cyclodextrin

Mono-6-iodo-6-deoxy-β-cyclodextrin was first synthesized as previously described.[2] To synthesize the mono-6-deoxy-6-methanethiosulfonyl-β-cyclodextrin derivative, a previous procedure was adapted.[3] To a solution of 0.5 g mono-6-iodo-6-deoxy-β-cyclodextrin in 5 mL DMF was added 72 mg $NaSSO_2CH_3$ and the mixture was stirred for 24 h at 50°C under reflux and N_2 atmosphere. The reaction mixture was concentrated in a vacuum to obtain a syrup-like mass, and 10 mL EtOH was added. The resulting solid was filtered, exhaustively washed with EtOH and dry under vacuum. Yield: 0.41 g (0.33 mmol). ^{1}H-RMN (DMSO-d6, 500 MHz): d = 2.42 (s, 3H), 2.95 (s, 3H), 3.20-3.67 (m, 40H), 4.16-4.20 (m, 1H), 4.32 (d, 1H), 4.37-4.39 (m, 1H), 4.45-4.48 (m, 2H), 4.52 (m, 3H), 4.77 (d, 2H), 4.84 (m, 5H), 5.64-5.85 (m, 14H). IR (KBr): 3527, 3360, 1651, 1020 cm^{-1}.

1.4. Preparation of solid S_0.[4]

Mesoporous silica nanoparticles (MSN) were prepared according to our previously adapted protocol.[4] Cetyltrimethylammonium bromide (1.0 g) was placed in a 1.0 L three-neck round-bottom flask, and 480 mL of double-distilled water were added. The surfactant was dissolved under sonication, and then 3.5 mL of 2.0 mol/L NaOH solution were added. The temperature of the mixture was adjusted to 80ºC and 5.0 mL tetraethoxysilane were added dropwise to the solution within 5 min under vigorous magnetic stirring. The mixture was allowed to react for 2 h. The resulting white solid was filtered, washed with water and methanol, and then dried in desiccator. To remove the surfactant template, the solid **S_0** was finally calcined at 550 ºC for 5 h.

In parallel, Au nanoparticles (20 nm) were prepared according to the Frens method[5] by heating 100 mL of 0.3 mM $HAuCl_4$ solution to boiling. Then, 5 mL of a 39 mM trisodium citrate solution were added and the mixture was heated for 10 min and further cooled to room temperature. This procedure was repeated four times to prepare the volume of Au nanoparticles required.

Au-MSN Janus nanoparticles were prepared according to our previously reported method.[4] Briefly, 200 mg MSN were dispersed in 10 mL of 1.0 μM of cetyltrimethylammonium bromide in 6.7% ethanol aqueous solution, and the mixture was heated at 75ºC. One gram of paraffin wax was added and the mixture was kept at 75ºC until the paraffin wax was melted. The mixture was vigorously stirred at 25000 rpm for 10 min using an Ultra Turrax T-18 homogenizer, and then stirred for 1 h at 4000 rpm and 75ºC using a magnetic stirrer. The resulting Pickering emulsion was then cooled to room temperature, mixed with 10 mL methanol and treated with 200 μL of (3-mercaptopropyl)trimethoxysilane. After 3 h under magnetic stirring, the silanized emulsion was filtered off, three-times washed with methanol and further dispersed in 400 mL of Au nanoparticles aqueous solutions. The mixture was stirred overnight, then filtered and washed two-times with ethanol, three-times with chloroform and dried overnight at 70ºC. The resulting solid **S_0** was exhaustively washed with ultrapure water, dried and kept in desiccators until use. Au-MSN Janus nanoparticles were prepared in good yield (56%), as revealed by TEM analysis. Au:MSN ratio in Janus nanoparticles

was estimated as 38%, 27%, 19% and 16% for 1:1, 2:1, 3:1 and +3:1 morphology, respectively.

1.5. Preparation of S_1.[4]

Solid $\mathbf{S_0}$ (100 mg) were dispersed in 5.0 mL MeOH and 100 µL 3-mercaptopropionic acid were added. The mixture was stirred for 1 h, then centrifuged and the solid was repeatedly washed with MeOH. The modified nanoparticle was further dispersed in 5.0 mL MeOH and mixed with 100 µL 3-mercaptopropyltrimethoxysilane. The mixture was stirred for 3 h at room temperature, then centrifuged and the solid was repeatedly washed with MeOH and finally dried in desiccator.

The modified nanoparticle (100 mg) and 60 mg of tris(2,2´-bipyridyl)ruthenium(II) chloride hexahydrate were suspended in 20 mL of anhydrous acetonitrile inside a round-bottom flask connected to a Dean-Stark trap under Ar atmosphere. The suspension was refluxed at 110 °C in azeotropic distillation, collecting about 4 mL in the trap in order to remove the adsorbed water. The mixture was stirred for 24 h at room temperature to load the dye into the MSN face pores. The resulting orange solid was filtered off, washed two times with 30 mL acetonitrile, and dried under Ar atmosphere.

Solid $\mathbf{S_1}$ was prepared by dispersing 50 mg of the dye-loaded solid in 5 mL of anhydrous toluene containing 100 mg t-BuOK. The suspension was stirred during 10 min, centrifuged and the solid was washed three times with anhydrous toluene. The solid was then dispersed in 3.0 mL DMF and mixed with 3.0 mL DMF containing 100 mg of mono-6-deoxy-6-methanethiosulfonyl-β-cyclodextrin. The mixture was stirred overnight, filtered off and sequentially washed with DMF, DMF:acetonitrile (1:1), acetonitrile and 100 mM sodium phosphate buffer, pH 7.0 until a clear solution is obtained. The solid $\mathbf{S_1}$ was then washed with ultrapure water, dried and kept in desiccators until use.

Tris(2,2´-bipyridyl)ruthenium(II) content was quantified by incubating 5 mg of solid $\mathbf{S_1}$ in 2 mL of 1 M NaOH during 1 h. The resulting solution was centrifuged and the absorbance at 454 nm was measured. In parallel, solutions of different concentrations of tris(2,2´-bipyridyl)ruthenium(II) in 1 M NaOH were treated under the same conditions to further construct a calibration plot for quantitative determination of the dye. All determinations were performed by triplicate.

1.6. Preparation of S_2.[4]

To prepare the solid $\mathbf{S_2}$, 20 mg of solid $\mathbf{S_1}$ were dispersed in 2.0 mL of cold 100 mM sodium phosphate buffer, pH 7.0 containing 10 mg 1-ethyl-3-(3-dimethylaminopropyl)carbodiimide (EDAC) and 10 mg N-hydroxysuccinimide (NHS). The mixture was stirred for 1 h at 4ºC and then 150 µg acetylcholine esterase were added. The mixture was stirred overnight at 4ºC, centrifuged and the solid was repeatedly washed with cold sodium phosphate buffer. The solid was then suspended in 5.0 mL of cold 10 mM sodium phosphate buffer, pH 10 and 2.0 mg Azure A hydrochloride were added. The

mixture was stirred overnight at 4ºC in dark conditions, then centrifuged and exhaustively washed with cold sodium carbonate buffer until a clear solution is obtained. Solid $\mathbf{S_2}$ was then dried and kept in refrigerator until use. The Azure A content was determined by sequential incubation of 5 mg of solid $\mathbf{S_1}$ in three portions of 1 mL of 1 M HCl, and further measurement of absorbance at 620 nm in the resulting extracted solution. Dye was quantified by using a proper calibration plot. All determinations were performed by triplicate.

1.7. Release assays.

In a typical release assay, 5 mg $\mathbf{S_2}$ were suspended in 5 mL of 20 mM Na_2SO_4 solution at pH 7.5 and shaken over time at 25ºC. After 60 min incubation, the enzyme substrates acetylcholine or acetylthiocholine were added to a final concentration of 150 mM. Aliquots were taken at scheduled times, centrifuged and the absorbance at 454 nm and 620 nm was measured to detect the released tris(2,2′-bipyridyl)dichlororuthenium(II) and Azure A, respectively. As control experiments, $\mathbf{S_2}$ samples were suspended in similar buffer solution without addition of triggers. Released dyes were quantified by using 14335 M^{-1} cm^{-1} and 57500 M^{-1} cm^{-1} and as extinction coefficients for tris(2,2′-bipyridyl)dichlororuthenium(II) and Azure A, respectively.[6,7] For control experiments, thermal inactivated samples were prepared by boiling a 1 mg/mL dispersion of solid $\mathbf{S_2}$ during 15 min, and further washing until a clear solution is obtained.

1. F. Worek, U. Mast, D. Kiderlen, C. Diepold and P. Eyer, *Clin. Chim. Acta*, 1999, **288**, 73.
2. L.D. Melton and K.N. Slessor, *Carbohydr. Res.*, 1971, **18**, 29.
3. B.G. Davis, R.C. Lloyd and J.B. Jones, *J. Org. Chem.*, 1998, **63**, 9614.
4. R. Villalonga, P. Díez, A. Sánchez, E. Aznar, R. Martínez-Máñez and J.M. Pingarrón, *Chem. Eur. J.*, 2013, **19**, 7889.
5. G. Frens, *Nat. Phys. Sci.*, 1973, **241**, 20.
6. W. DeWilde, G. Peeters and J.H. Lunsford, *J. Phys. Chem.*, 1980, **84**, 2306.
7. P. Paul, S.S. Mati, S.C. Bhattacharya and G.S. Kumar, *Phys. Chem. Chem. Phys.,* 2017, 19, 6636.